Optical Engineering

SPIEDigitalLibrary.org/oe

Novel algorithm to compensate nonlinear response of photo detector to improve quality of image reconstruction for compressed sensing

Jiayan Zhuang
Qian Chen
Weiji He
Weiyi Feng

SPIE

Novel algorithm to compensate nonlinear response of photo detector to improve quality of image reconstruction for compressed sensing

Jiayan Zhuang
Qian Chen
Nanjing University of Science and Technology
Nanjing, Jiangsu 210094, China
E-mail: cq1964@163.com

Weiji He
Jiangsu Key Lab of Spectral Imaging & Intelligence Sense (SIIS)
Nanjing, Jiangsu 210094, China

Weiyi Feng
Nanjing University of Science and Technology
Nanjing, Jiangsu 210094, China

Abstract. In imaging systems based on compressed sensing, error in the measured data is incurred due to the nonlinear response of the photo detector, which affects the quality of the reconstructed images. We propose an algorithm to compensate the nonlinear response from the detector. The compensation is based on the detector response curve on the measured data. The theoretical analysis and simulation results show that this algorithm can greatly reduce the reconstruction errors caused by the detector's nonlinear response. Furthermore the peak signal-to-noise ratio of the reconstructed image and the system reconstruction rate have been significantly improved, while the fine feature of the images is better preserved and reconstructed as compared to that without using the algorithm. [DOI: 10.1117/1.OE.52.4.043204]

Subject terms: compressed sensing; detector response; nonlinear system; imaging processing.

Paper 121829 received Dec. 13, 2012; revised manuscript received Mar. 21, 2013; accepted for publication Mar. 25, 2013; published online Apr. 18, 2013.

1 Introduction

Compressed sensing has been proposed for several years.[1] The technique has been greatly improved and widely used for imaging systems,[2–4] such as the single-pixel camera by Duarte[5] and the complicated three-dimensional imaging system. The imaging systems mentioned above fully reflect the advantage of compressed sensing for faster imaging processing time without complicated mechanical scanning structure.

When a system of image reconstruction is based on compressed sensing, the system will inevitably produce various types of errors affecting the image quality. The nonlinear response from the detector is one of the main contributors to the errors.[6–8] To correct the error due to the nonlinear response for compressed sensing, Tao et al. have done a series of studies with the following results:[9,10]

Assume the measured value y can be expressed as

$$y = \Phi x \tag{1}$$

during the ideal reconstruction process. Here $\Phi(M, N)$ is a Gaussian random measurement matrix for compressed sensing, M is the number of the measured data points while N is the length of the one-dimensional original signal. x is the original input signal. The reconstruction error can be expressed as

$$\|\hat{x} - x\|_2 = \|\Delta x\|_2 \le C_1\eta, \tag{2}$$

where $\hat{x}$ is the reconstructed signal, Δx is the difference between the reconstructed signal and the original signal, while C_1 and η are both positive constants. When there are errors, such as the measurement error and the quantization error, note the errors as e, $\|e\|_2 \le \sigma$, where σ is a positive constant. Then, the measured value y for a nonideal system can be expressed as

$$y = \Phi x + e. \tag{3}$$

The reconstruction error can be written as[9]

$$\|\hat{x} - x\|_2 \le C_1\eta + C_2\sigma, \tag{4}$$

where C_2 is a positive constant. Before using compressed sensing to reconstruct the original signal, the system first needs to obtain a set of measured values modulated by the Gaussian matrix. The measured values directly affect the accuracy of the reconstructed signal. When the imaging system detects the input signal using a photo-detector, the detector nonlinear response may impact the accuracy of the measured values, degrading the quality of the final reconstructed images. Furthermore, it may also significantly impact the imaging system recovery efficiency.

When the detector has a nonlinear response error ζ ($\|\zeta\|_2 \le \varsigma$, where ς is a positive constant), the measured data can be expressed as

$$y = \Phi x + e + \zeta. \tag{5}$$

The expression below will be approved in this paper

$$\|\hat{x} - x\|_2 \le C_1\eta + C_2\sigma' \le C_1\eta + C_2\sigma + C_2\varsigma, \tag{6}$$

where σ' is a positive constant. Conventionally, the image reconstruction does not take into consideration the nonlinear response for compressed sensing.[11,12] When the detector presents nonlinearity, which is true for any real system, the image quality is impacted. Based on the above considerations, in order to improve the reconstructed image quality

and the robustness of the system, a new algorithm for detector nonlinear response compensation is proposed in this paper for compressed sensing. This new algorithm can reduce the response errors and increase the efficiency of the imaging system noticeably based on the theoretical analysis[13] and numerical simulation.[14]

2 Imaging System Based on Compressed Sensing

The imaging system used for discussion is the single-pixel camera, same as the one described in Ref. 5. The single-pixel camera imaging system is one of the representative imaging systems based on compressed sensing.[3] The system block diagram is shown in Fig. 1.

As in Fig. 1, the reflected optical light modulated by the DMD is received by the photo-detector. The measured data from the detector are fed into the computer. If the photo-detector has a nonlinear response, the measured data will be nonlinear, thus the reconstruction result will be impacted. So a nonlinearity compensation algorithm can be used for image reconstruction to improve the quality.

3 Algorithm of Detector Nonlinear Response Compensation

This section outlines the algorithm in theory in compensating the nonlinear response from the detector for imaging system based on compressed sensing. It also analyzes the reconstruction error affected by the nonlinear response.

3.1 *Nonlinear Response of the Detector*

In the theory of compressed sensing,[5] the measured values can be expressed as Eq. (1). In an experiment, the DMD pattern should be changed by M times to obtain different measured values. Giving y and the measurement matrix Φ, the reconstructed signal $\hat{x}$ is obtained by

$$\hat{x} = \underset{x}{\operatorname{argmin}} \|x\|_1 \ \text{s.t.} \| \Phi x - y \|_2 < \varepsilon, \tag{7}$$

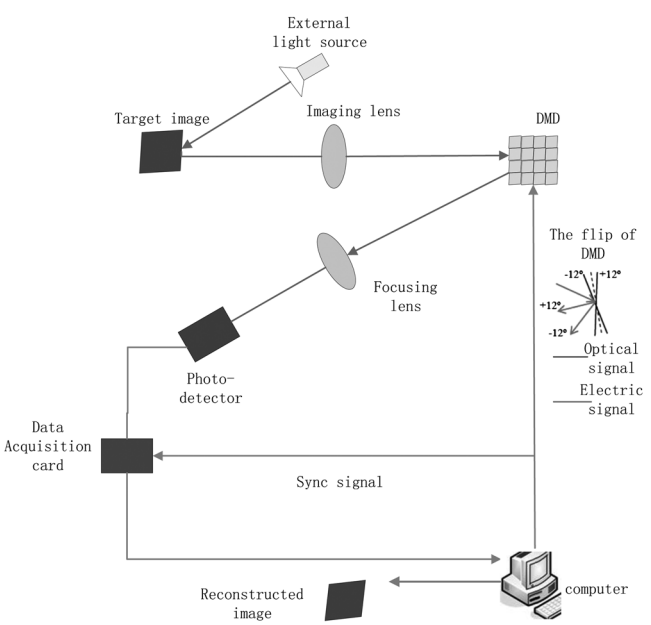

Fig. 1 System block diagram.

where ε is a positive constant. The measured values y can be expressed as

$$\begin{bmatrix} \Phi_{1,1}\Phi_{1,2}\ldots\Phi_{1,N} \\ \Phi_{2,1}\Phi_{2,2}\ldots\Phi_{2,N} \\ \ldots \\ \Phi_{M,1}\Phi_{M,2}\ldots\Phi_{M,N} \end{bmatrix} \cdot \begin{bmatrix} x_1 \\ x_2 \\ x_3 \\ \ldots \\ x_N \end{bmatrix} = \begin{bmatrix} y_1 \\ y_2 \\ y_3 \\ \ldots \\ y_M \end{bmatrix}. \tag{8}$$

When the detector response is linear and ξ is the response factor, from Eq. (8) it can be derived that

$$\begin{bmatrix} \Phi_{1,1}\Phi_{1,2}\ldots\Phi_{1,N} \\ \Phi_{2,1}\Phi_{2,2}\ldots\Phi_{2,N} \\ \ldots \\ \Phi_{M,1}\Phi_{M,2}\ldots\Phi_{M,N} \end{bmatrix} \cdot \begin{bmatrix} x_1 \\ x_2 \\ x_3 \\ \ldots \\ x_N \end{bmatrix} = \begin{bmatrix} \xi y_{1\xi} \\ \xi y_{2\xi} \\ \xi y_{3\xi} \\ \ldots \\ \xi y_{M\xi} \end{bmatrix}, \tag{9}$$

where $y_{i\xi}$ is the measured data after extracting the fixed response factor. Re-write the right side of the Eq. (9) as

$$\xi \cdot \begin{bmatrix} y_{1\xi} \\ y_{2\xi} \\ y_{3\xi} \\ \ldots \\ y_{M\xi} \end{bmatrix} = \begin{bmatrix} y_1 \\ y_2 \\ y_3 \\ \ldots \\ y_M \end{bmatrix}. \tag{10}$$

It can be seen from the Eq. (10) that when the detector response is linear, the measured data are a linear transformation. By removing the corresponding response factor, the original measured data are recovered and there is no nonlinear error in the image reconstruction.

When the detector response is nonlinear, note each response coefficient of the measured data as $\xi_1, \xi_{2,\ldots}, \xi_M$, respectively (excluding $\xi_1 = \xi_{2,\ldots,} = \xi_M$), then the measured data can be expressed as

$$\begin{bmatrix} \Phi_{1,1}\Phi_{1,2}\ldots\Phi_{1,N} \\ \Phi_{2,1}\Phi_{2,2}\ldots\Phi_{2,N} \\ \ldots \\ \Phi_{M,1}\Phi_{M,2}\ldots\Phi_{M,N} \end{bmatrix} \cdot \begin{bmatrix} x_1 \\ x_2 \\ x_3 \\ \ldots \\ x_N \end{bmatrix} = \begin{bmatrix} \xi_1 y_{1\xi_1} \\ \xi_2 y_{2\xi_2} \\ \xi_3 y_{3\xi_3} \\ \ldots \\ \xi_M y_{M\xi_M} \end{bmatrix}$$

$$= \xi_1 \cdot \begin{bmatrix} y_{1\xi_1} \\ \frac{\xi_2}{\xi_1} y_{2\xi_2} \\ \frac{\xi_3}{\xi_1} y_{3\xi_3} \\ \ldots \\ \frac{\xi_M}{\xi_1} y_{M\xi_M} \end{bmatrix}, \tag{11}$$

in which $y_{i\xi_i}$ is the measured data after extracting a fixed response factor. From Eq. (11), by extracting the smallest response factor (assume ξ_1 is the smallest one), it is observed that the measured data are a nonlinear transformation due to the nonlinear response of the detector. When the measured data are changed, it also leads to the decrease of reconstruction efficiency.

Equation (7) can be expressed as

$$\sqrt{(\Phi_1 x_1 - y_1)^2 + (\Phi_2 x_2 - y_2)^2 + \ldots + (\Phi_M x_M - y_M)^2} < \varepsilon. \tag{12}$$

For each measurement

$$|\Phi_i \hat{x}_i - y_i| = \varepsilon i' (\varepsilon i' \geq 0), \tag{13}$$

where $\hat{x}_i$ is the reconstructed signal from Eq. (12), $\varepsilon i'$ is a positive constant.

Assuming $\Phi_i \hat{x}_i - y_i \geq 0$, then Eq. (13) can be written as

$$\Phi_i \hat{x}_i = (\varepsilon_i' + y_i). \tag{14}$$

When $\Phi_i \hat{x}_i - y_i \leq 0$, a similar one to Eq. (13) can be derived. When the measured data are obtained, $\Phi_i \hat{x}_i$ can be expressed as Fig. 2.

Therefore,

$$(\varepsilon_i' + y_i) = |\Phi_i||\hat{x}_i| \cos\theta, \tag{15}$$

where θ is the angle of vector Φ_i and vector $\hat{x}_i$.

Generally speaking, $\Phi_i \hat{x}_i > 0$ (as shown in Fig. 2) and the probability of $\Phi_i \hat{x}_i = 0$ is very small. For example, when the target picture is all black, which means the pixel values are all 0, then $\Phi_i \hat{x}_i = 0$. Therefore such a scenario is excluded in discussion. When $\Phi_i \hat{x}_i \neq 0$, $|\hat{x}_i| \neq 0$, it is evident that $|\Phi_i| \neq 0$ & $\cos\theta \neq 0$.

Rewrite Eq. (15) as

$$|\hat{x}_i| = (\varepsilon_i' + y_i)|\Phi_i|^{-1} \cos\theta^{-1}. \tag{16}$$

When the nonlinearity is considered, Eq. (16) becomes

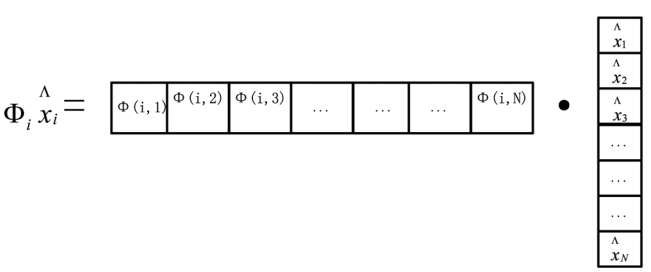

Fig. 2 Schematic diagram of $\Phi_i \hat{x}_i$.

$$|\hat{x}_i'| = |\Phi_i|^{-1} \cos\theta^{-1}(\varepsilon_i' + y_i'), \tag{17}$$

where y_i' is the nonlinear measured data.

Assume x_i as the original signal. From above, it can be derived that

$$|\hat{x}_i'| = |\Phi_i|^{-1} \cos\theta^{-1} \left| \left(\varepsilon_i' + \frac{\xi_i}{\xi_1} y_i \right) \right| \tag{18}$$

and

$$\Delta x = ||x_i| - |\hat{x}_i'|| = |\Phi_i|^{-1} \cos\theta^{-1} \left| \frac{\xi_i}{\xi_1} y_i - y_i + \varepsilon_i' \right| = |\Phi_i|^{-1} \cos\theta^{-1} \left| \frac{\xi_i - \xi_1}{\xi_1} \right| |y_i| + |\Phi_i|^{-1} \cos\theta^{-1} \varepsilon_i', \tag{19}$$

in which $\xi_i \geq \xi_1$. It can be seen from Eq. (19) that the nonlinear error in the measured data can directly lead to the reconstruction error. When the effect of the nonlinear response becomes noticeable, which means $|\xi_i - \xi_1|$ is large, the construction error rate increases, thereby degrading image quality. Therefore, it is very important to compensate the nonlinear response for the detector, which is this paper's focus.

Let $e + \zeta = e'$, $\|e'\|_2 \leq \sigma'$, then $y = \Phi x + e + \zeta$, which can be further expressed as $y = \Phi x + e'$. Therefore,

$$\|\hat{x} - x\|_2 \leq C_1 \eta + C_2 \sigma' \tag{20}$$

as

$$\|e'\|_2 = \|e + \zeta\|_2 \leq \|e\|_2 + \|\zeta\|_2 \leq \sigma + \varsigma \tag{21}$$

so that

$$\|\hat{x} - x\|_2 \leq C_1 \eta + C_2 \sigma' \leq C_1 \eta + C_2 \sigma + C_2 \varsigma. \tag{22}$$

In the above, $C_2\varsigma$ is the reconstruction error due to nonlinear response from the detector. As shown in Figs 3–5, the detector nonlinear response apparently affects the quality of the reconstructed images, so $C_2\varsigma$ needs to be minimized.

3.2 *Algorithm to Compensate Nonlinear Response from the Detector*

It is well known that the photo-detector response model function can be briefly expressed as

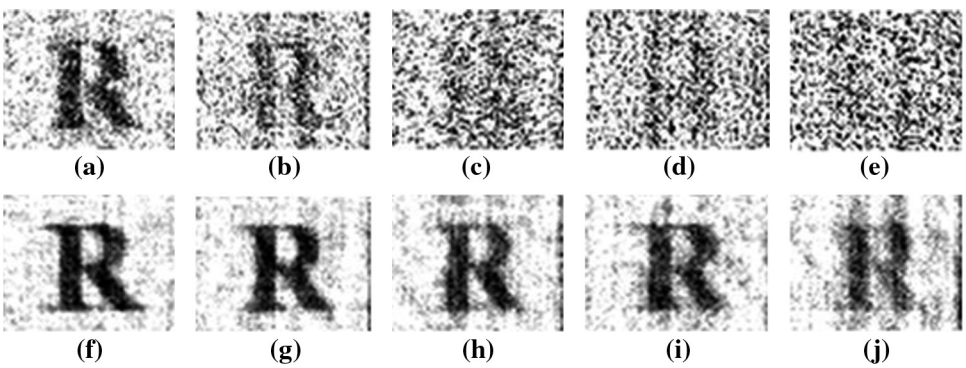

Fig. 3 The simulation of Picture R.

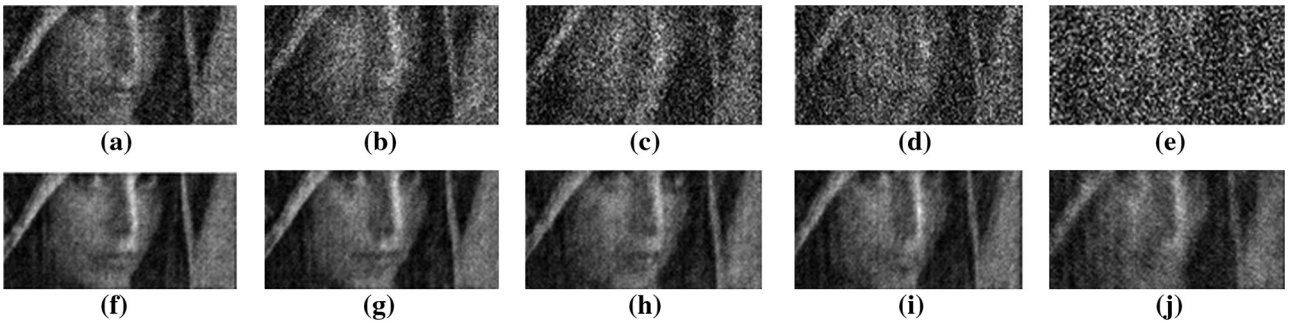

Fig. 4 The simulation of Picture Lena.

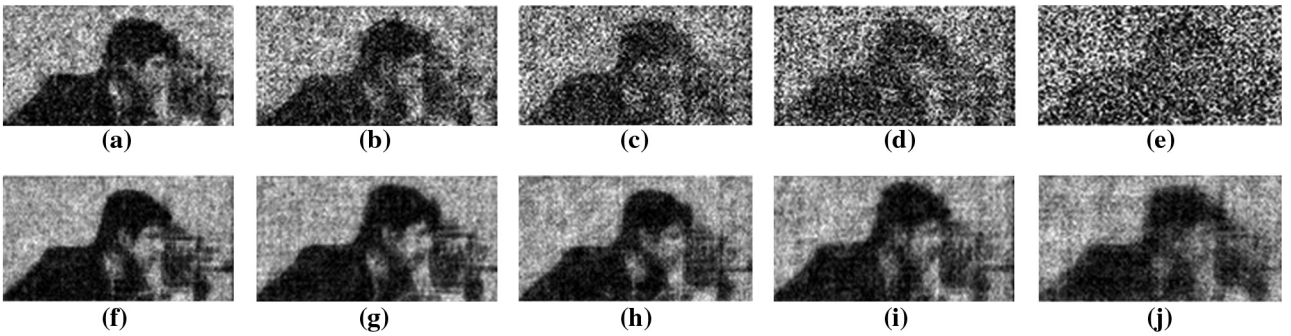

Fig. 5 The simulation of Picture Camera.

$$y = f(I) + b. \tag{23}$$

In Eq. (23), b represents the accuracy error of the linear measurement. b is part of the imaging error. I represents the incident light intensity. f is the detector response function.

Suppose the linear detection range of the detector is $I_{\min} < I < I_{\max}$. When $I \geq I_{\max}$ or $I \leq I_{\min}$, it can be seen that the measured data y are in a nonlinear state. Therefore, compensation on the nonlinearity becomes necessary.

The process of the compensation algorithm is as shown in Fig. 6.

Figure 6 depicts detector response curve, in which ξ is the detector response factor. If the detector response factor does not change for a given region, then this region can be treated as a linear detection region. Otherwise, it is nonlinear.

Measured data associated with the nonlinear region in Fig. 6 is rejected in the algorithm. The data corresponding to the linear region is described below.

Assume M is the total number of the measured data points while m is the number of the measured data points in the nonlinear response region. Define an operation

$$y(j) = \begin{cases} \text{keep } y(i), & \text{if } y(i) \text{ in the linear region} \quad j = 1, 2, \ldots, M - m \\ \text{reject } y(i), & \text{if } y(i) \text{ in the nonlinear region} \quad i = 1, 2, \ldots, M \end{cases}. \tag{24}$$

The dimension of the measured data is $M - m$ after the rejection.

Since both the measured data and the Gaussian random measurement matrix are needed for signal reconstruction and each measured data has its corresponding Gaussian random measurement matrix, therefore after changing the measured data, the Gaussian random measurement matrix should also have the appropriate operation before the final recovery.

Let the Gaussian random measurement matrix be $\Phi(M, N)$. In the measured data matrix y, $y(i)$ corresponds to the Gaussian random measurement matrix $\Phi(i, N)$. When $y(i)$ is rejected, the Gaussian random measurement matrix should also be changed accordingly as

$$\Phi(j, N) = \begin{cases} \text{keep } \Phi(i, N), & \text{if } y(i) \text{ in the linear region} \quad j = 1, 2, \ldots, M - m \\ \text{reject } \Phi(i, N), & \text{if } y(i) \text{ in the nonlinear region} \quad i = 1, 2, \ldots, M \end{cases}. \tag{25}$$

Figure 7 is the schematic diagram demonstrating the compensation process of the measured data and the Gaussian random measurement matrix.

In fact, there is no such ideal linear detection. The linear detection region shown in the Fig. 6 is actually an approximation. The response factor also changes in this region but does not change significantly. Such a region is called

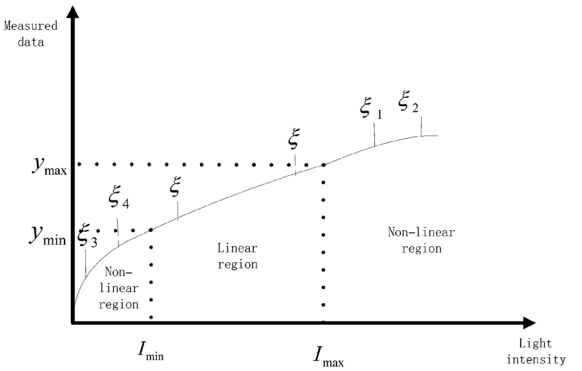

Fig. 6 Detector response curve.

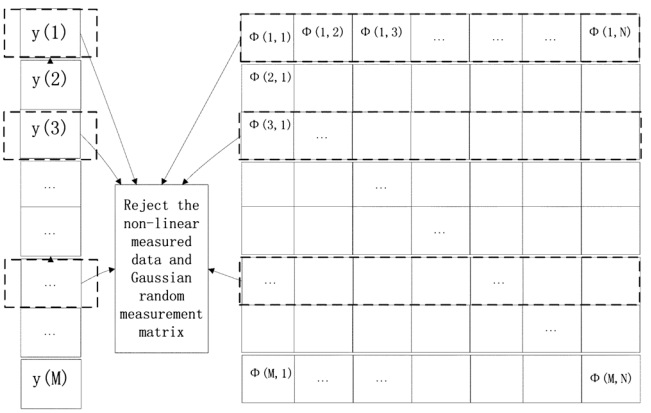

Fig. 7 Correction of the measured data and the Gaussian random measurement matrix.

a near-linear region. The next section is the process to compensate the measured data in the near-linear region in order to get the reconstructed image with improved equality.

As shown in Fig. 8 the near-linear region is divided into P equal parts, where P is a positive integer. The boundary of the region is noted as $y_{\max}$ and $y_{\min}$. $y_{\max}$ is the largest measured data in the near-linear region while $y_{\min}$ is the smallest. The interval of the adjacent parts is $(y_{\max} - y_{\min})/P$. The average response factor $\xi_{i\text{average}}$ of each divided part is $\xi_{i\text{average}} = [(y_{i+1} - y_i)/(I_{i+1} - I_i)] \quad (i = 1, 2, 3, \ldots,)$. The measured data are assigned for each divided part according to the numerical size and the number of the measured value points that each part C_i has is determined. The part with the

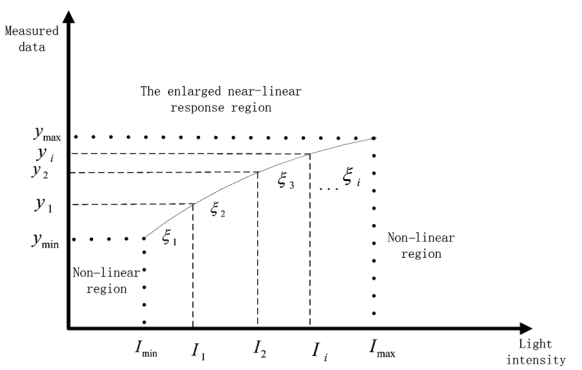

Fig. 8 Near-linear region of the detector response curve.

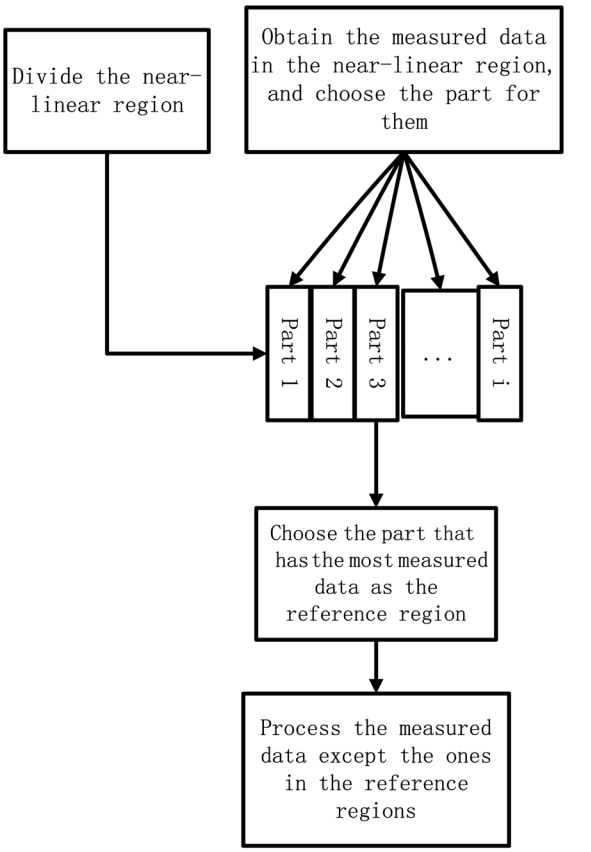

Fig. 9 Compensation flow for the near-linear region.

largest number of data points is the reference region. The average response factor of the reference region will be the reference response factor ξ' and the measured data of the other regions are processed as below

$$y_i'' = \frac{y_i}{\xi_{i\text{average}}} \cdot \xi'. \tag{26}$$

In Eq. (26), ξ' is the reference response factor; $\xi_{i\text{average}}$ is the average response factor of the region C_i; y_i is the measured data in the region C_i, and y_i'' is the measured data which have been compensated by the response reference factor. Figure 9 illustrates compensation flow for the near-linear region.

Finally, an $M - m$ dimensional measured data matrix is obtained with the improved recovery image for compressed sensing. The overall block diagram of the algorithm proposed in this paper is illustrated in Fig. 10. In short, when obtaining the measured data, data corresponding to the nonlinear region are rejected and the corresponding Gaussian random measurement matrix is modified. Data in the near-linear region are used for processing based on the algorithm proposed here to get the reconstructed image with improved quality for compressed sensing.

3.3 *Theoretical Analysis of the Algorithm on Error Reduction*

Assume y_i' is the measured data under the ideal linear detection; y_i'' is the measured data after processing, and y_i is the measured data that have not been processed.

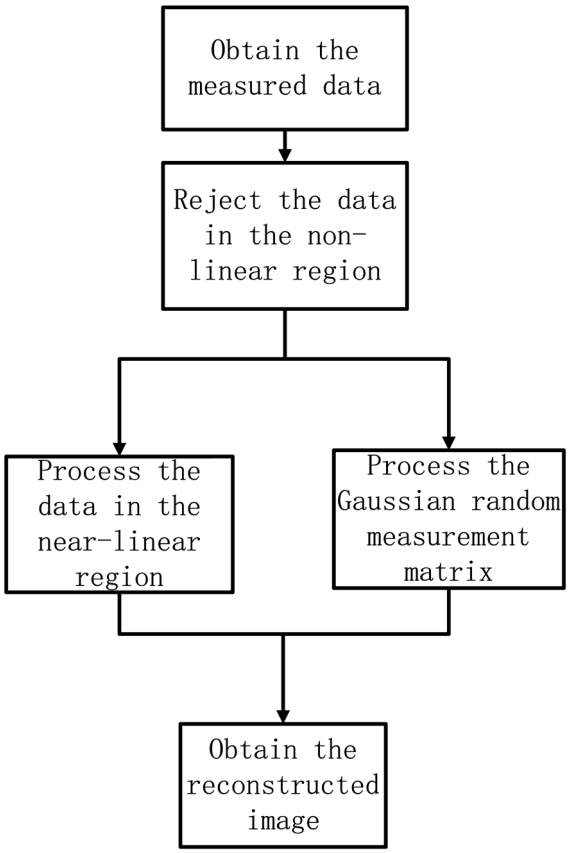

Fig. 10 Block diagram of the correction algorithm.

Correspondingly, ξ_i is the response factor of y_i; ξ' is the reference response factor; and $\xi_{i\text{average}}$ is the average response factor of the region C_i as defined in the previous sections.

The ideal measured data that are linear can be expressed as

$$y_i' = \frac{y_i}{\xi_i} \cdot \xi'. \tag{27}$$

The measured data after the compensation can be shown as Eq. (26).

If it can be proved that

$$|y_i'' - y_i'| \ll |y_i - y_i'|, \tag{28}$$

it means that the measured data through the compensation using the algorithm by this paper are with less error or better image quality.

Using the above expressions, it can be derived that

$$|y_i'' - y_i''| = y_i \xi' \left| \frac{\xi_{i\text{average}} - \xi_i}{\xi_i \xi_{i\text{average}}} \right|, \tag{29}$$

$$|y_i - y_i'| = y_i \xi_{i\text{average}} \left| \frac{\xi_i - \xi'}{\xi_i \xi_{i\text{average}}} \right|. \tag{30}$$

By extracting the common divisor $y_i/\xi_i\xi_{i\text{average}}$, Eqs. (29) and (30) become

$$|y_i'' - y_i'| = \xi' |\xi_{i\text{average}} - \xi_i| \cdot \frac{y_i}{\xi_i \xi_{i\text{average}}}, \tag{31}$$

$$|y_i - y_i'| = \xi_{i\text{average}} |\xi_i - \xi'| \cdot \frac{y_i}{\xi_i \xi_{i\text{average}}}. \tag{32}$$

The following description consists of two main parts: Part A and Part B. It is outlined previously that the near-linear response curve has a stationary nonlinear factor rate R. Generally speaking, we can also assume the nonlinear factor will not change too much in the near-linear region. So in this section it is assumed $|\xi_{i\text{average}} - \xi'|/(\xi' \ll 1)$.The stationary nonlinear factor rate can be written as

$$R = \frac{\Delta\xi}{\Delta y}, \tag{33}$$

where Δy is the changing rate of the measured data and $\Delta\xi$ is the changing rate of the nonlinear response factor. Nonlinear rate shows the number of the measured data in the nonlinear region. The threshold value will be set to determine whether the measured data are in the nonlinear region or not. The nonlinear rate is

$$S\prime = \frac{N_{y_{\text{non}}}}{M_{y_M}}. \tag{34}$$

$N_{y_{\text{non}}}$ is the number of the measured data points in the nonlinear detection region and M_{y_M} is the number of the whole measured data points. The nonlinear factor rate shows the changing rate of the nonlinear factor. The larger the nonlinear factor rate is, the more nonlinear the measured data will be.

- Part A: $\xi_i > \xi'$

Figure 11 shows the scenario of $\xi_i > \xi'$. When $\xi_i > \xi'$, for the majority of the measured data, it is a valid assumption that

$$|\xi_i - \xi'| > |\xi_{i\text{average}} - \xi_i|, \qquad \xi_{i\text{average}} > \xi'. \tag{35}$$

Please note that the measured data farther from the reference region are very effective when applying the

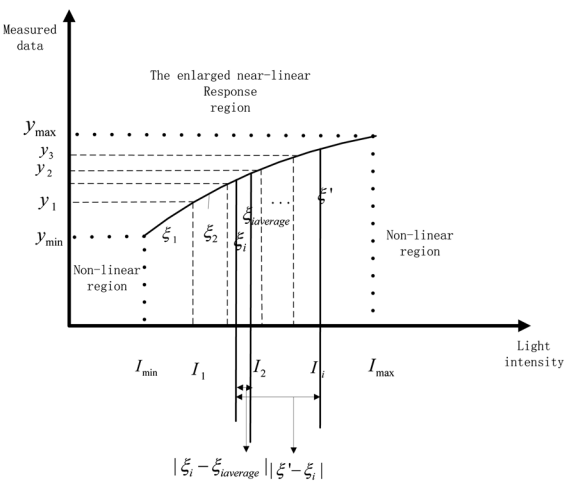

Fig. 11 $\xi_i > \xi'$ in the near-linear region.

compensation. There are few measured data points that are very close to the reference region. For those data, the compensation effectiveness may not be good, but it will not impact the overall effectiveness of the compensation.

From Eq. (35) it can be obtained that

$$\xi'|\xi_{i\text{average}} - \xi_i| \xi_{i\text{average}}|\xi_i - \xi'|, \tag{36}$$

which means the measured data after compensation are closer to the ideal case, which is linear.

- Part B: $\xi_i < \xi'$ and $\xi_i = \xi'$

With the above assumption and Fig. 11, it can be easily derived that for the majority of the measured data, below is a valid assumption

$$\frac{|\xi_i - \xi'|}{|\xi_{i\text{average}} - \xi_i|} > \frac{\xi'}{\xi_{i\text{average}}}. \tag{37}$$

From Eq. (37)

$$\xi'|\xi_{i\text{average}} - \xi_i| \xi_{i\text{average}}|\xi_i - \xi'|, \tag{38}$$

when $\xi_i = \xi'$.

The probability of $\xi_i = \xi'$ is small, and it has very little effect on the reconstruction when this event happens. So the case of $\xi_i = \xi'$ is not considered here.

From the above discussion, when there is a nonlinear response error ζ, where $\zeta = \zeta_1 + \zeta_2$, ζ_1 is the error of the nonlinear response and ζ_2 is the error of the near-linear response, the measured data can be expressed as

$$y = \Phi x + e + \zeta. \tag{39}$$

Assume $\|\zeta\|_1 \le \varsigma_1$, $\|\zeta\|_2 \le \varsigma_2$, after the compensation, ζ_1 can be ignored and ζ_2 is also reduced. Therefore,

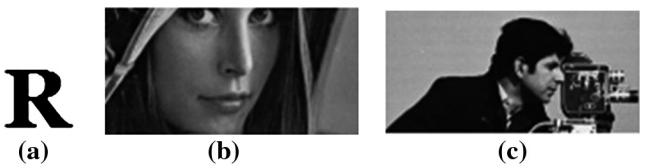

Fig. 12 Target images.

$$\|e'\|_2 = \|e + \zeta\|_2 \le \|e\|_2 + \|\zeta\|_2 \le \|e\|_2 + \|\zeta_1 + \zeta_2\|_2 \le \|e\|_2 + \|\zeta_1\|_2 + \|\zeta_2\|_2 \le \sigma + \varsigma_1 + \varsigma_2 = \sigma + \varsigma_2, \tag{40}$$

together with Eq. (4)

$$\|\hat{x} - x\|_2 \le C_1\eta + C_2\sigma' = C_1\eta + C_2\sigma + C_2\varsigma_2. \tag{41}$$

After the compensation, $C_2\varsigma_1$ can be ignored and $C_2\varsigma_2$ is reduced, which means the reconstruction error has been minimized with better image quality.

4 System Simulation

4.1 *Definition of Parameters*

The sampling rate is defined as

$$S = \frac{M}{N}, \tag{42}$$

where M is the number of the measured data points and N is the length of the one-dimensional original signal. The sampling rate shows the number of measured data points. The larger the sampling rate is, the more measured data obtained and the better the reconstructed result will be. The peak signal-to-noise ratio (PSNR) and M-rate (also called the reconstruction rate) are as in Refs. 15 and 16:

$$\text{PSNR} = 10 * \log\ 10[255^2 * N/(\|x - x'\|_2)^2], \tag{43}$$

$$M - \text{rate} = 1 - \sqrt{\frac{\sum_1^n [x(i) + x'(i)]^2}{\sum_1^n [x(i) - x'(i)]^2}}, \tag{44}$$

where x is the gray value of the original image and x' is the gray value of the image after compensation.

4.1.1 *Simulation results*

The target images to be simulated are the Picture R, Picture Lena, and Picture Camera as shown in Fig. 12. The resolution of Picture R is 64×48, and the resolution of Picture Lena and Picture Camera are both 128×64.

Figures 3–5 give the comparison between the reconstructed images with and without using the compensation algorithm. The sampling rate is 30%. The nonlinear rate

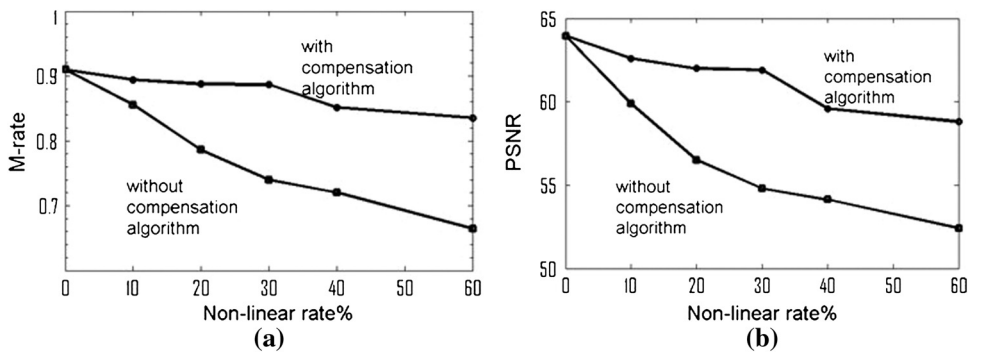

Fig. 13 PSNR and the reconstruction rate of R.

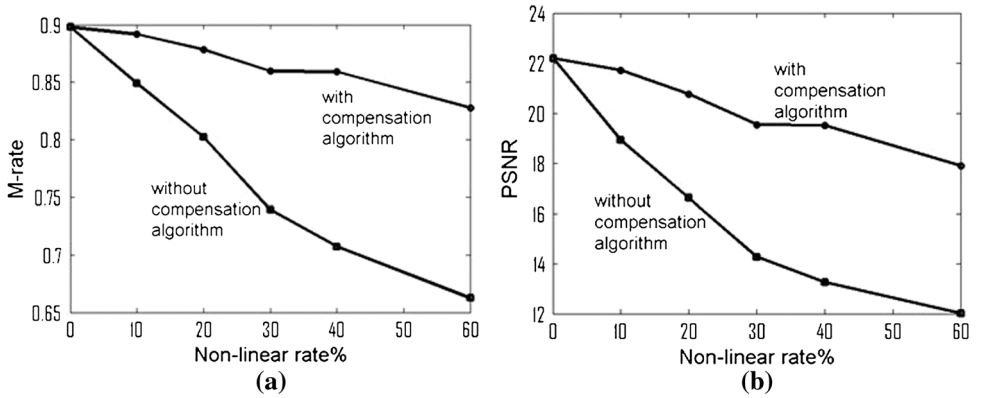

Fig. 14 PSNR and the reconstruction rate of Lena.

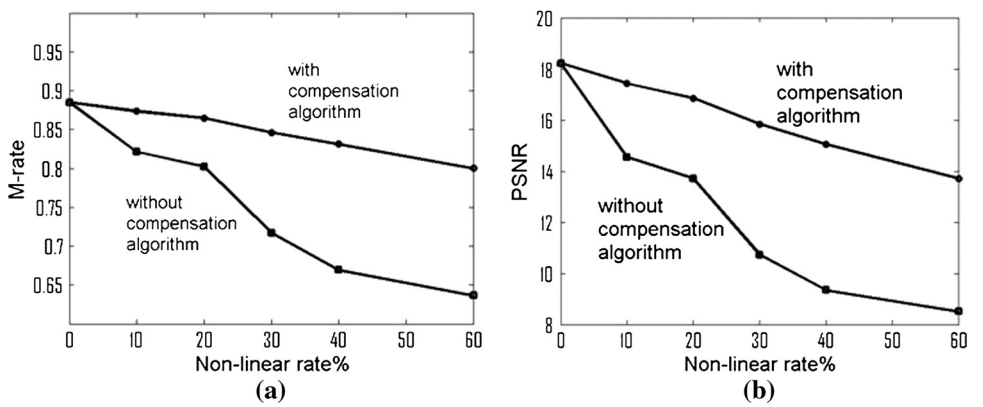

Fig. 15 PSNR and the reconstruction rate of Camera.

S' of the five different comparisons is 10%, 20%, 30%, 40%, and 60%, from the left to the right.

The simulation for Picture R is shown in Fig. 3. Figure 3(a)–3(e) shows the reconstruction results without the compensation algorithm. Figure 3(f)–3(j) shows the reconstruction results with the compensation algorithm.

In simulation, the nonlinear factor rate used is 0.025, and the near-linear region of the measured data is divided into six parts. It can be seen that the compensation algorithm significantly improves the quality of image reconstruction.

Figure 4 is the simulation of Picture Lena. In the simulation, the nonlinear factor rate is 0.0025. It is found that the more complex the pictures are, the worse the reconstructed pictures will be due to the nonlinear response. In order to compare the reconstructed pictures with and without using the compensation algorithm, the nonlinear factor rate is reduced to 0.0025. The near-linear region of the measured data is divided into six parts. As shown in Fig. 4, the compensation significantly improves the image quality.

Figure 4(a)–4(e) shows the reconstruction results without the compensation algorithm. Figure 4(f)–4(j) shows the reconstruction results with the compensation algorithm.

Similar assumption is used for the simulation of Picture Camera and the same observation in improving the image quality is obtained. For simplicity, it will not be repeated here.

Figure 5(a)–5(e) shows the reconstruction results without the compensation algorithm. Figure 5(f)–5(j) shows the reconstruction results with the compensation algorithm.

Figures 13–15 give the values of the PSNR ratio and the reconstruction rate of the pictures of Picture R, Picture Lena, and Picture Camera.

From the above analysis, it can be seen that after using the nonlinear compensation algorithm, the PSNR ratio and the reconstruction rate of the images have been significantly improved to mitigate the impact of the nonlinearity from the detector. The algorithm reduces the error caused by the detector nonlinearity and improves the imaging efficiency of the system as well.

5 Conclusion

In the imaging system based on compressed sensing, the detector nonlinear response incurs reconstruction error and degrades image quality and imaging efficiency. In order to resolve the issue, a compensation algorithm is proposed in this paper. Theoretical analysis and simulation show that the proposed algorithm can effectively mitigate the impact caused by the nonlinear response from the detector. The reconstruction efficiency and PSNR ratio have also been significantly improved after the compensation.

It is unknown whether rejecting the measured data will succeed for the situation of too many measured data in the nonlinear region. This can be future work for continuous improvement.

Acknowledgments

This project is sponsored by the National Natural Science Foundation of China (NSFC) (Grant Nos. 61101196,

61271332, and 61177091), Weaponry Pre-research Project (Grant No. 40405080401), and National Postdoctoral Foundation (Grant No. 2012M521085).

References

1. Y. Tsaig and D. L. Donoho, "Extensions of compressed sensing," Technical Report, Department of Statistics, Stanford University (2004).
2. L. Li et al., "Gated viewing laser imaging with compressive sensing," *Opt. Soc. Am.* **51**(14), 2706–2712 (2012).
3. L. I. Shen, M. A. Cai-wen, and X. I. A. Ai-li, "Optical imaging based on compressive sensing," *Proc. SPIE* **8194**, 81942H (2011).
4. D. Keming et al., "Photon-counting imaging system based on compressive sensing," *Infrared Laser Eng.* **41**(2), 363–368 (2012).
5. M. F. Duarte et al., "Single-pixel imaging via compressive sampling," *IEEE Signal Process. Mag.* **25**(2), 83–91 (2008).
6. J. N. Laska et al., "Democracy in action: Quantization, saturation, and compressive sensing," *Applied and Computational Harmonic Anal.* **31**(3), 429–443 (2011).
7. T. Blumensath and M. E. Davies, "Iterative hard thresholding for compressed sensing," *Appl. Comput. Harmonic Anal.* **27**(3), 265–274 (2009).
8. H. T. Kung, T.-H. Lin, and D. Vlah, "Identifying bad measurements in compressive sensing," in *Proceedings of IEEE Conference on Computer Communications Workshops (INFOCOM WKSHPS)*, Shanghai, China, pp. 1054–1059 (2011).
9. E. Candes, J. Romberg, and T. Tao, "Stable signal recovery from incomplete and inaccurate measurements," *Commun. Pure and Appl. Math.* **59**(8), 1207–1223 (2006).
10. E. Candes, J. Romberg, and T. Tao, "Robust uncertainty principles: Exact signal reconstruction from highly incomplete frequency information," *IEEE Trans. Infom. Theory* **52**(2), 489–509 (2006).
11. W. Lu, "Compressed sensing and sparse signal processing," Technical Report, Department of Electrical & Computer Engineering, University of Victoria, Canada (2004).
12. Software:l1-magic, http://www.dsp.ece.rice.edu/cs.
13. Y. Zhu, L. Rao, and T. Yan, *The Analysis, and Calculation of Matrix*, 1st ed., Chinese National Defence Industry Press, Beijing, China (2010).
14. Y. Wu, P. Ye, and I. O. Mirza, "Experimental demonstration of an optical sectioning compressive sensing microscope (CSM)," *Opt. Express* **18**(24), 24565–24578 (2010).
15. C. G. Lee, I. Moon, and B. Javidi, "Photon-counting three-dimensional integral imaging with compression of elemental images," *Opt. Soc. Am.* **29**(6), 854–860 (2012).
16. Y. Liu and R. Zhao, "Matching pursuit algorithm for signal reconstruction based on compressive sensing," Master's Thesis Fulltext Database (CMFD), Beijing Jiaotong University, China (2010).

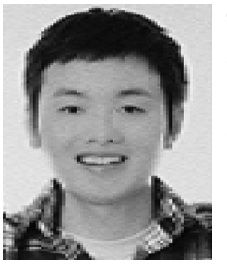

Jiayan Zhuang is pursuing his PhD in engineering at the School of Electronic and Optical Engineering at Nanjing University of Science and Technology. His research interests include nonlinear imaging processing, optical applications of compressed sensing, and biomedical imaging.

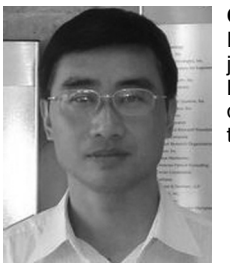

Qian Chen is a professor at the School of Electronic and Optical Engineering at Nanjing University of Science and Technology. His research interests include photoelectric detection, image processing, and photoelectric signal processing.

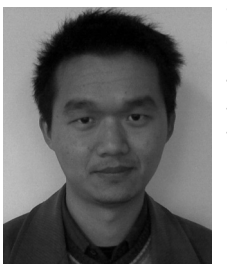

Weiji He is a lecturer of the Jiangsu Key Lab of Spectral Imaging and Intelligence Sense (SIIS) at Nanjing University of Science and Technology. His research interests include the mechanism and application of photoelectric detection.

Weiyi Feng: biography and photograph not available.